Experimental and Numerical Investigations on the Bearing Capacity of Footings on the Layered Soil

Avinash Bhardwaj[1] · Ravi Kumar Sharma[1]

Abstract

Model footing tests were conducted on two types of footings having aspect ratio (L/B) equals to 1, and 2 resting on single and two layered soil with a geogrid layer placed at the interface of two layered soil. The effect of the upper soft clayey layer stabilized with molasses, waste foundry sand, and lime over medium dense sand was studied by varying the thickness ratio (h/B) of upper layer ($h/B = 0.8, 1.2, 1.6, 2.0$). The reinforcement effect was investigated by adding geogrid layer of varying width ratio ($b/B = 0, 2, 3, 4$) at the interface between upper soft/stabilized clayey layer and lower medium dense sand layer. In order to validate the results of the model plate load tests, the bearing capacity behaviour of footings with aspect ratios (L/B) of 1 and 2 was calculated using the finite element method (FEM)-based ABAQUS software. The results of model plate load tests shows that the ultimate bearing capacity of square and rectangular shaped footings at $h/B = 1.6$ and $b/B = 3$ was optimum when compared to other thickness ratios (h/B) and width ratios (b/B). This is because the above soft clayey soil was stabilised with optimum amount of additives and placement of a geogrid layer at the interface. Further, upon comparing the pressure settlement behaviour curves generated using model plate load tests and ABAQUS software, a close agreement was found, with numerical results rising slightly upwards.

Introduction

Foundation is an essential geotechnical structure that distributes weight from the superstructure to the underlying soil without shear. There are four main conditions that must be met for a foundation to be considered good: it must be secure against the complete collapse or failure of the soils upon which it is founded; it must not experience excessive settlements or movements; environmental, soil type, ground water table and seismic activity factors must be properly considered; and the foundation must be economically feasible in relation to the function and cost of the overall structure. Regardless of the foundation's purpose, these requirements are always followed. However, the primary requirement is that the foundation must be safe against possible instability.

Soil plays a major role in determining the depth of the foundation required to keep a building stable [1–4]. Different kinds of soil will require different type of foundations. This means that the soils underneath the foundation must be strong enough to support the weight of the building.

Expansive soils are foundation material that alters volume due to changes in soil moisture [5, 6]. These type of soils are typically found in the world's dry and semi-arid regions. Expansive soil represent about 20% of the land area in India and may be found in large parts of the Deccan Plateau, Andhra Pradesh, Karnataka, Madhya Pradesh, Maharashtra, and Gujarat [7]. Because of the strong swelling pressure imposed by these soils, lightweight buildings are badly harmed [8]. During the construction of the Rajasthan canal (now Indira Gandhi Nahar) in India, it was reported that bentonite exists beneath the dune sand or at depth while the canal is in cutting. This produces swelling (volume change) and, as a result, breaches in the canal lining [9]. The annual cost of damage to the civil engineering structures is estimated at several lakhs of rupees in India [10]. The swelling and shrinking characteristics of expansive soils cause damage to buildings and result

✉ Avinash Bhardwaj
avinash@nith.ac.in

Ravi Kumar Sharma
ravi@nith.ac.in

1   Civil Engineering Department, NIT Hamirpur, Hamirpur, HP 177005, India

in a loss of more than 9 billion dollars annually in the United States alone [11, 12]. In year 1992, it was estimated that the United Kingdom lost around £150 million due to structural damage caused by expansive soils [13], while in 2012, the cost was estimated at over £400 million [14]. As a result, it is essential to verify the soil properties for safe building operations and cost-effective designs.

In order to reinforce expansive soil, improvements that every geotechnical engineer aims to enhance include enhancing the load bearing capacities, tensile strength, and overall performance of in-situ subsoil. Soil stabilisation is a remedial strategy that lowers the permeability and compressibility of the soil mass in earth structures, increases its shear strength, and aids in the reduction of structural settlement. Many soils with poor geotechnical characteristics were modified in past using soil stabilization technique by adding waste foundry sand, construction demolition waste, glass waste, fibers, waste iron etc. [15–22].

In the past three decades, geogrid has been employed as reinforcement in the construction of many earth-retaining and earth-supported structures [23, 24]. Reinforcement and separation are the primary functions of geogrid. Geogrid-reinforced buildings utilize less concrete, less labour and less construction time compared to traditional concrete buildings. By using less concrete, they contribute to a reduction in carbon emissions associated with concrete production, which is a significant source of greenhouse gas emissions [25]. Model plate load tesets were performed on clayey soil stabilized with lime (3, 6, and 12 percent), geotextile reinforcement, geocell reinforcement, geosynthetics reinforcement, and geosynthetics reinforcement with lime stabilization at different rates [26–29]. It was revealed that improving the soil with lime and then reinforcing it with geosynthetics gives better results on these types of soils.

There has been very little research conducted in past on the bearing capacity characteristics of clayey soils (C) treated with molasses (M), waste foundry sand (WFS), and lime (L) alone and in combination with each other. Triaxial testing, UCS, and CBR make up the majority of the experimental work in author's previous work [15]. These tests provide only indirect information on the geotechnical properties of clayey soil. Model studies are often less expensive and have the advantage of allowing variables to be examined under controlled situations. Model testing, if carried out appropriately, might be advantageous in certain cases. Model testing gives valuable quantitative data that may be used to analyze the effect of critical variables on prototype tests. Keeping in view the research gap, the objective of the present study was focused on to investigate the effect of soft/stabilized clayey soil overlying medium dense sand with or without geogrid layer placed at the interface of layered soil on the mechanical behavior and failure mechanism of footings having aspect ratio (*L/B*) equal to 1 and 2 using experimental and numerical approach.

Materials Used

The disturbed soil samples were taken from the side of NH-88 (Kangra- Shimla route) near the Jukhala village in the Bilaspur district of Himachal Pradesh, India. After sample collection in airtight bags, samples were transported to the laboratory. The pulverization of soil samples has been done in the pulverizing machine after drying the soil samples (Fig. 1) and then again sealed in air-tight bags to avoid any variation in moisture content. The soil has been classified as clayey soil of high plasticity (CH) according to Unified Soil Classification System (USCS). Table 1 and Fig. 2 presents the geotechnical characteristics and particle size
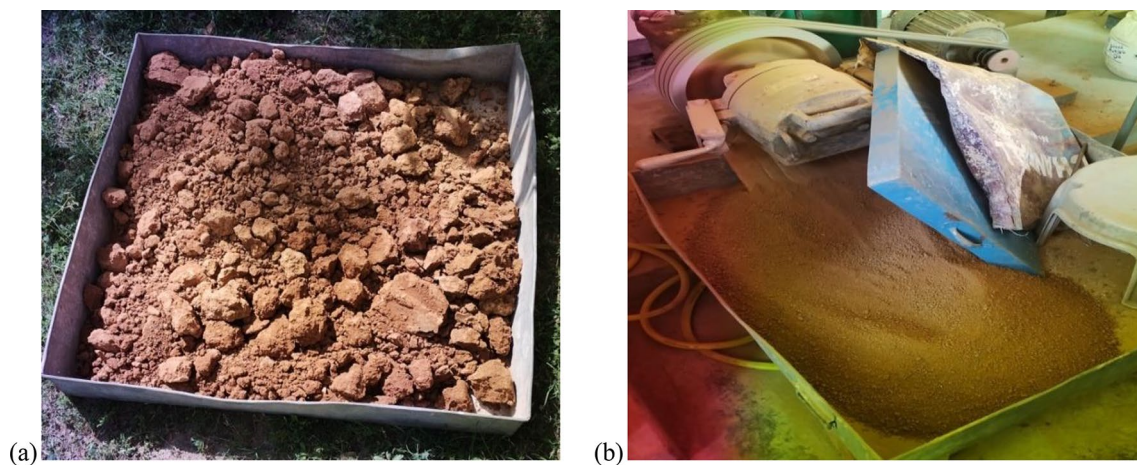

Fig. 1 (**a**) Drying under natural sunlight and; (**b**) pulverization process of soft clayey soil

Table 1 Geotechnical properties of clayey soil, WFS, and sand

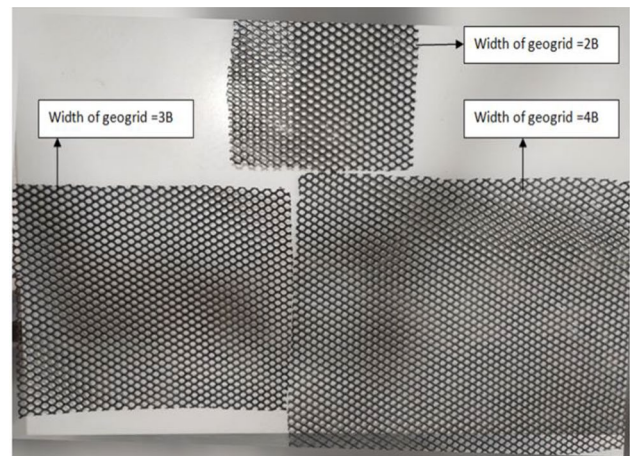| Soil properties	Clay	WFS	Sand
Soil type [31]	CH	SP	SP
Liquid limit [34]	55%	–	–
Plastic limit [34]	20%	–	–
Plasticity index	35%	–	–
Specific gravity [35]	2.6	2.64	2.65
Differential free swell index [36]	35%	–	–
Optimum moisture content [37]	16.5%	8.20%	–
Maximum dry unit weight [37]	17.1 kN/m^3	15.9 kN/m^3	16.2 kN/m^3

Fig. 3 Biplanar geogrid

distribution curve of the soft clayey soil investigated in the research, respectively.

Molasses used in the study was obtained from Budhewal Co-Operative Sugar Mill Ltd., located in the Punjab region of Ludhiana. The waste foundry sand used in this work is a recycling waste from Shakti Foundries in Ludhiana (Punjab). WFS have a dark colour and a sandy texture due to the angular shape of the waste particles and the fines that are adhered to the sand particles. Dry sieve analysis in accordance with [30] gave the gradation curve for WFS. The effective size (D10), coefficient of curvature (Cc) and coefficient of uniformity (Cu) for the sand are 0.14 mm, 0.89 and 1.44 respectively, indicating that WFS is poorly graded in nature, with the majority of the particles falling into the fine sand range. Table 1 and Fig. 2 presents the geotechnical characteristics and particle size distribution curve of the WFS used in this study. Hydrated lime utilized in this investigation was purchased from a hardware store in Hamirpur, Himachal Pradesh. The geogrids used in this research was purchased from Suntech geotextile private limited, New Delhi and are made from a coextruded composite polymer sheet that was perforated and orientated (Fig. 3).

Three different dimensions of biplanar geonet was used in the present study having width ratios (*b/B*) equal to 2, 3, and 4 (where, *b* = width of geogrid and *B* = width of footing). The final structure was made up of hexagon aperture geometries formed by continuous and non-continuous ribs. Table 2 lists the physical and mechanical characteristics of geogrid used in the model plate load tests which were provided by the distributor. Sand used in the model plate load test program has been obtained from geotechnical engineering laboratory, in civil engineering department of National Institute of Technology Hamirpur, H.P. India. The sand is classified as SP (poorly graded sand) according to the Unified Soil Classification System [31]. As determined by [32] and [33], the maximum and minimum dry unit weights of sand are 16.2 kN/m^3 and 13.2 kN/m^3, respectively, while the minimum and maximum void ratios are 0.61 and 0.9, respectively. The effective size (D10), coefficient of curvature (Cc) and coefficient of uniformity (Cu) for the sand are 0.16 mm, 0.88 and 1.43 respectively. Table 1 and Fig. 2

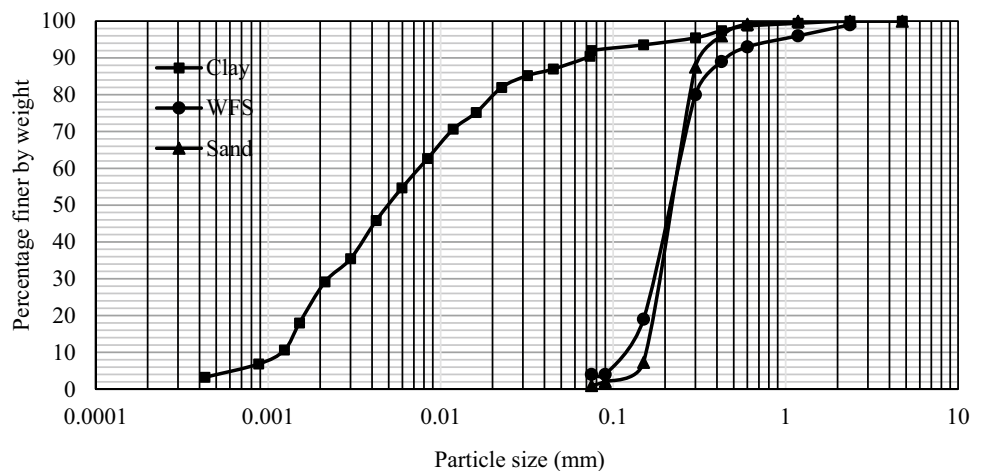**Fig. 2** Particle size curve for clayey soil, WFS, and sand

**Table 2** Physical and mechanical properties of geogrid

Property	Type or value
Mesh type	Biplanar
Colour	Black
Polymer type	HDPE
Packaging	Rolls
Roll width	2 m
Roll length	30 m
Unit mass	650 g/m^2
Tensile strength	7.20 kN/m
Percentage elongation at maximum load	20.2%

presents the geotechnical characteristics and particle size distribution curve of the medium dense sand used in the research, respectively.

Testing Program

When undertaken with greater care, model plate load tests are more suited than full-scale prototype testing, both economically and technically. All model testing were carried out in accordance with [38]. The model footings were made of mild steel and were resized, thickened (25 mm), and shaped (square and rectangular) to the necessary dimensions. To eliminate boundary effects, a minimum of 500 mm (5 times the width of the footing) of space was allowed in all directions from the footing's edges [38]. A testing tank with inner dimensions of 700 mm long, 500 mm wide, and 600 mm deep was used to prepare the soil bed. The size of the testing tank was chosen in consideration of the size of the footing and its zone of impact [38]. The dimensions of shallow square and rectangular shaped footing were 100 mm × 100 mm ($L/B = 1$), 100 mm × 200 mm ($L/B = 2$) respectively. Universal testing machine installed in geotechnical laboratory in civil engineering department of National Institute of Technology, Hamirpur (H.P.) India was used to conduct the model plate load tests. A testing tank, universal testing machine, model plates, and dial gauges make up a model plate load testing equipment. In Fig. 4, a schematic diagram of the testing assembly is presented.

This study will look into two different primary scenarios. In the first situation, it was assumed that the foundation was supported by a single layer of soil, and in the second case foundation was resting on two layers of soil. The one layer system in the first situation was supposed to be sandy soil with footing overlays on medium dense sand. In second situation, it was assumed that the soft clay/stabilized clay layer placed on top of the sandy soil and the footing was resting on top of the soft clay/stabilized clay. Designation and details of type of soil placed in single layer and two layered soil are shown in Table 3 for both types of footings. Combinations
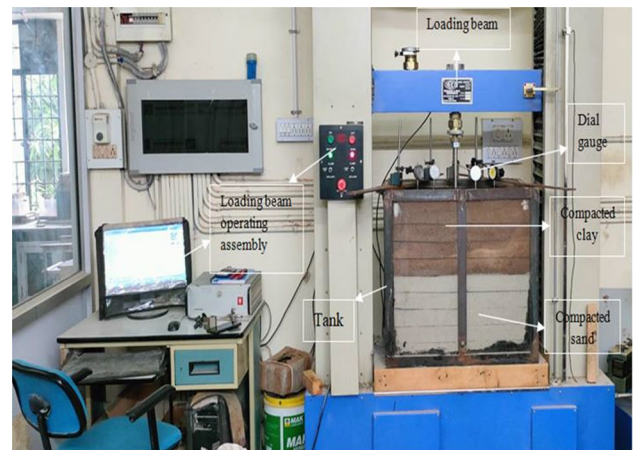
Fig. 4 Overall test set up for model plate load tests

used in the present study were taken from author's previous work [15]. Table 4 shows the details of total number of model plate load tests performed in the present study.

Preparation of Bed

Sand raining technique was used to fill one layer of medium-dense sand to an appropriate density and then leveled after the desired height had been reached in single layer and two layered soil. For two layered soil, thickness of the upper layer varied and it was depending on the thickness ratio (h/B) adopted for the particular model plate load test. For layered soil, the bed was made up of two layers of soft / stabilized clayey soil overlying over medium dense sand. First, the bottom medium dense sand layer was filled at a known and appropriate density using the rainfall technique, and then leveled after reaching the required height (Fig. 5a). Second, if the test supposed was to be with a geogrid layer then a layer of biplanar geonet placed before placing the soft/ stabilized clayey soil layer above the medium dense sand layer (Fig. 5a) and if it was without a geogrid layer then soft/stabilized clayey soil layer was directly compacted with the help of rammers over medium dense sand (Fig. 5b, c). A manually operated rammer used in compaction test [37] was used for the compaction of upper layer as the tank size being small. To achieve the desired density each layer was compacted with around 400 blows uniformly with the same compaction energy.

Results and Discussion

The pressure-settlement curves obtained after conducting model plate load test, on all the parameters under study, are shown in Figs. 6, 7, 8, 9, 10, 11, 12, 13. Bearing capacity results obtained from model plate load tests for cases 2–9

Table 3 Designation and details for model plate load tests and numerical modeling [15]

Designation	Soil type in single and two layered soil		Maximum dry unit weight (kN/m³)	Modulus of elasticity (E) (MPa)	Poisson ratio (ν)	Angle of internal friction (ϕ)	Cohesion (c) (kN/m²)
Case 1	Single layer	Medium dense sand	16.15	32.3	0.3	35	0.1
Case 2	Upper layer	Unstabilized clay	17.10	3.2	0.3	14.86	21.77
	Lower layer	Medium dense sand	16.15	32.3	0.3	35	0.1
Case 3	Upper layer	Stabilized clay (C:M:90:10)	17.90	5.3	0.3	9.6	10.3
	Lower layer	Medium dense sand	16.15	32.3	0.3	35	0.1
Case 4	Upper layer	Stabilized clay (C:WFS: 80:20)	17.81	7.2	0.3	19.11	19.08
	Lower layer	Medium dense sand	16.15	32.3	0.3	35	0.1
Case 5	Upper layer	Stabilized clay (C:L:91:9)	16.06	9.6	0.32	21.43	17.61
	Lower layer	Medium dense sand	16.15	32.3	0.3	35	0.1
Case 6	Upper layer	Stabilized clay (C:M:WFS:80:10:10)	18.40	10.3	0.33	23.62	16.43
	Lower layer	Medium dense sand	16.15	32.3	0.3	35	0.1
Case 7	Upper layer	Stabilized clay (C:M:L:84:10:6)	17.50	14.7	0.34	25.64	15.59
	Lower layer	Medium dense sand	16.15	32.3	0.3	35	0.1
Case 8	Upper layer	Stabilized clay (C:WFS:L:74:20:6)	17.30	16.2	0.36	27.85	14.78
	Lower layer	Medium dense sand	16.15	32.3	0.3	35	0.1
Case 9	Upper layer	Stabilized clay (C:M: WFS:L: 67:10:20:3)	18.20	18.5	0.38	29.68	13.89
	Lower layer	Medium dense sand	16.15	32.3	0.3	35	0.1

Table 4 Details of total number of model plate load tests performed

Designation	Aspect ratio, (L/B)	Thickness ratio, (h/B)	Width ratio, (b/B)	No. of tests
Case 1	1, 2	–	–	2
Case 2–9	1, 2	0.8, 1.2, 1.6, 2.0	0, 2, 3, 4	256
Grand total				258

were compared with case 1 and is treated as the reference case. It's important to note that if the definite peak in the curve is visible, the ultimate bearing capacity is equal to the peak pressure. If the peak pressure in the plot could not be found, the ultimate bearing capacity was calculated using the double tangent method or the minimum of the bearing capacities that matched at least 10% of the width of footing ($B = 100$ mm).

Effect of additives, varying thickness ratio (h/B) of the upper layer, geogrid width, and footing type on bearing capacity are studied using non-dimensional factor improvement factor (IF). IF is the ratio of the ultimate bearing capacity (UBC) of a footing resting on unreinforced medium dense sand to the ultimate bearing capacity of footing resting on layered soil (soft/stabilized clayey soil overlying medium dense sand with or without a geogrid layer). In current investigation IF for square ($L/B = 1$) or rectangular ($L/B = 2$) shaped footings may be defined as the ratio of UBC

observed for cases 2–9 to the UBC observed for case 1. The results of model plate load testing are presented in depth in subsequent sections with respect to the following variables.

Effect of Varying Thickness Ratio (h/B) and Additives on UBC and IF

Effect of varying thickness ratio (h/B) of cases 2–9 at $b/B = 0$ on the bearing capacity of footings ($L/B = 1, 2$) of case 1 (reference case) has been discussed in this section.

Figures 6, 7 shows the pressure-settlement curves at $h/B = 0.8$ for both footings ($L/B = 1, 2$) for cases 2 and 9 compared with case 1. From these Figs. it was observed that bearing capacity of square and rectangular shaped footings declined to 112 kN/m² and 103 kN/m² for case 2 and it increased to 208 kN/m² and 197 kN/m² respectively for case 9. For case 2 at $h/B = 0.8$ the improvement factor (IF) of both footings ($L/B = 1, 2$) are 0.65 and 0.67 respectively

(a) Placement of geogrid above leveled sand bed

(b) Compaction and filling of clayey soil in tank and metal cups

(c) Placement of dial gauges at a distance of l =1.5B and 2.5B from footing centre on both sides, (l= distance of gauges from footing centre)

(d) Placement of square model footing (*L/B*=1) above leveled clayey layer bed

Fig. 5 Preparation of model plate load test set up
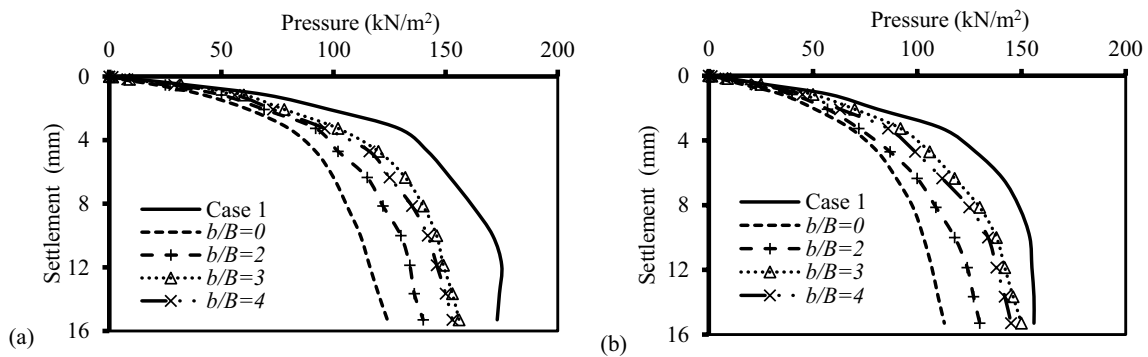
Fig. 6 Pressure-settlement curves at *h/B*=0.8 of case 2 with or without geogrid compared with case 1; (**a**) *L/B*=1, (**b**) *L/B*=2

and for case 9 IF rises to 1.22 and 1.28, resulting in a 21% and 28% rise in ultimate bearing capacity (UBC) for both footings respectively when compared with the reference case (Fig. 14).

Figures 8, 9 shows the pressure-settlement curves at *h/B*=1.2 for both footings (*L/B*=1, 2) for cases 2–9

compared with case 1. From these Figs. it was observed that bearing capacity of square and rectangular shaped footings declined to 86 kN/m^2 and 80 kN/m^2 for case 2 and it increased to 245 kN/m^2 and 229 kN/m^2 respectively for case 9. For case 2 at *h/B*=1.2 the improvement factor (IF) of both footings are 0.5 and 0.52 and for case 9 IF rises to 1.43 and
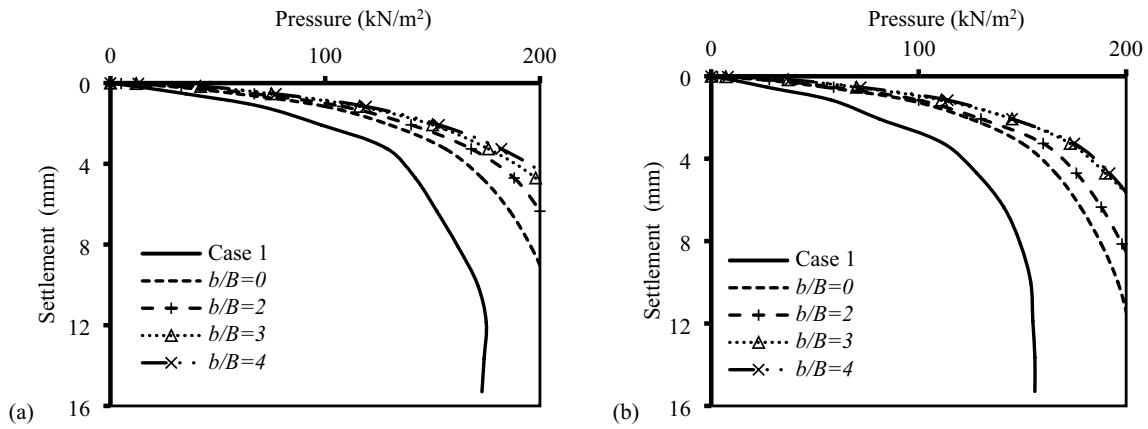
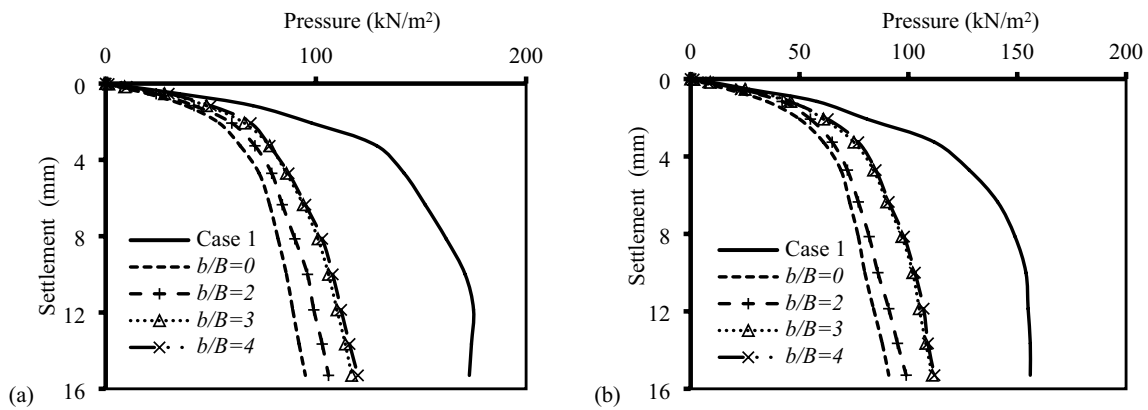**Fig. 7** Pressure-settlement curves at $h/B = 0.8$ of case 9 with or without geogrid compared with case 1; (**a**) $L/B = 1$, (**b**) $L/B = 2$

Fig. 8 Pressure-settlement curves at $h/B = 1.2$ of case 2 with or without geogrid compared with case 1; (**a**) $L/B = 1$, (**b**) $L/B = 2$
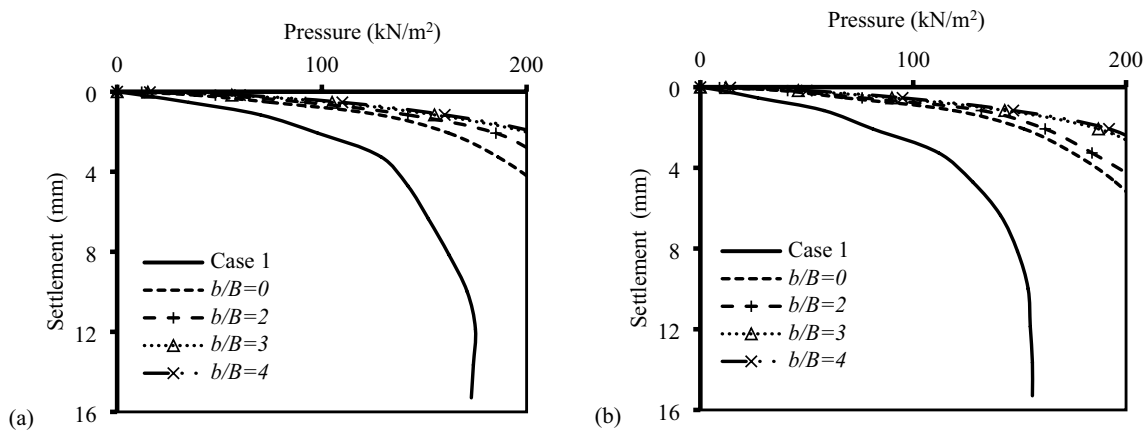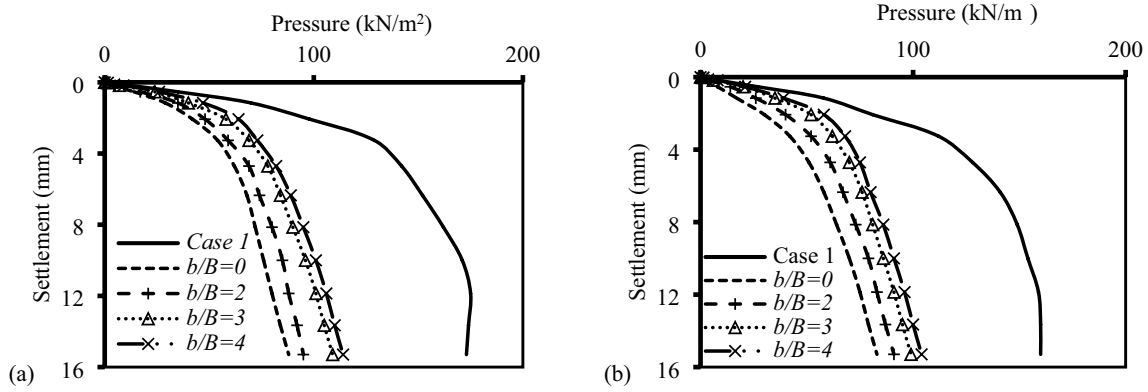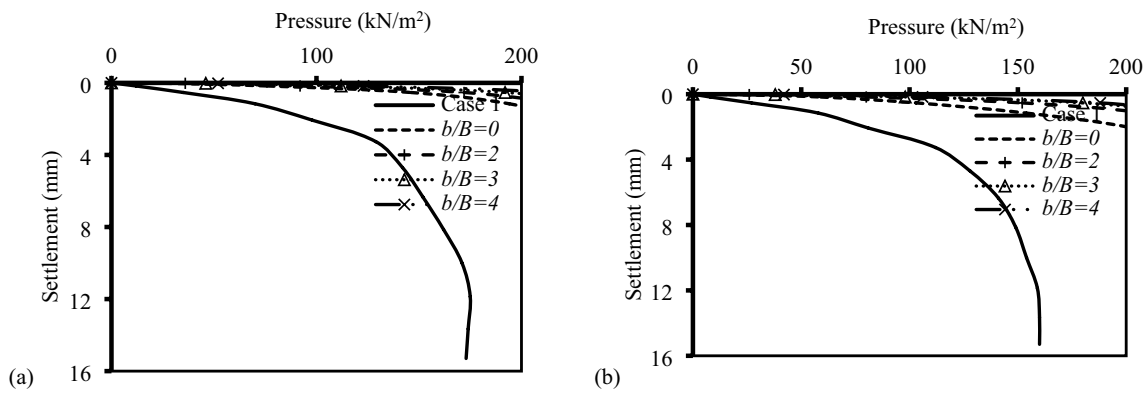
Fig. 9 Pressure-settlement curves at $h/B = 1.2$ of case 9 with or without geogrid compared with case 1; (**a**) $L/B = 1$, (**b**) $L/B = 2$
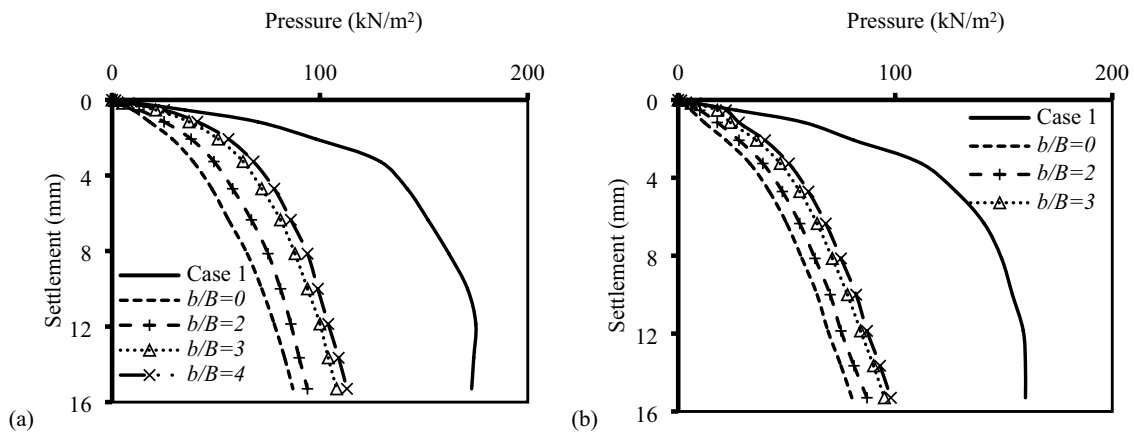
1.49 respectively, resulting in a 43% and 48% rise in ultimate bearing capacity (UBC) for both footings respectively when compared with the reference case (Fig. 14).

Figures 10, 11 shows the pressure-settlement curves at $h/B = 1.6$ for both footings ($L/B = 1, 2$) for cases 2–9 compared with case 1. From these Figs. it was observed that

Fig. 10 Pressure-settlement curves at $h/B = 1.6$ of case 2 with or without geogrid compared with case 1; (**a**) $L/B = 1$, (**b**) $L/B = 2$

Fig. 11 Pressure-settlement curves at $h/B = 1.6$ of case 9 with or without geogrid compared with case 1; (**a**) $L/B = 1$, (**b**) $L/B = 2$

Fig. 12 Pressure-settlement curves at $h/B = 2.0$ of case 2 with or without geogrid compared with case 1; (**a**) $L/B = 1$, (**b**) $L/B = 2$

bearing capacity of square and rectangular shaped footings declined to 76 kN/m² and 70 kN/m² for case 2 and it increased to 314 kN/m² and 287 kN/m² respectively for case 9. For case 2 at $h/B = 1.6$ the improvement factor (IF) of both

footings are 0.44 and 0.45 and for case 9 IF rises to 1.84 and 1.86 respectively, resulting in a 83% and 86% rise in ultimate bearing capacity (UBC) for both footings respectively when compared with the reference case (Fig. 14).
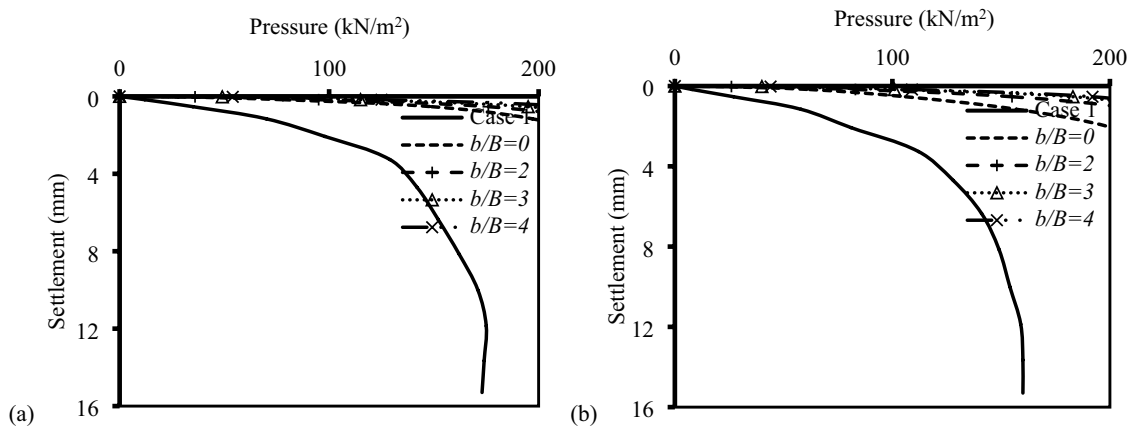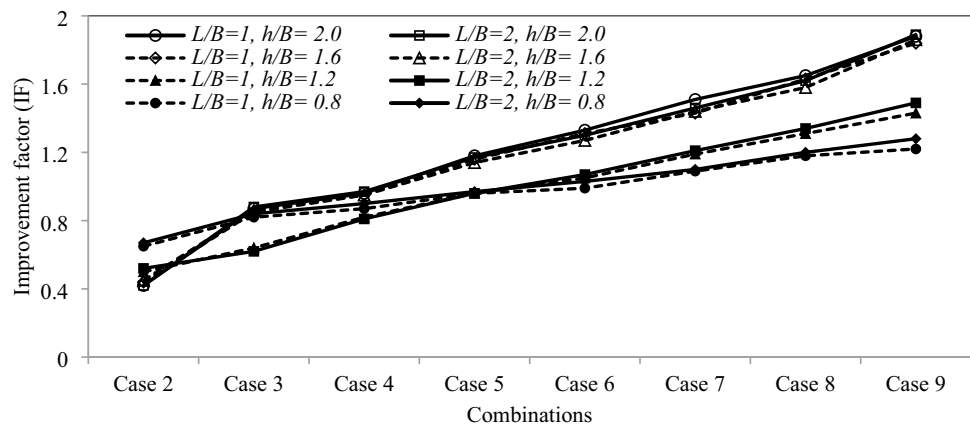
Fig. 13 Pressure-settlement curves at $h/B=2.0$ of case 9 with or without geogrid compared with case 1; (**a**) $L/B=1$, (**b**) $L/B=2$

Fig. 14 Variations in IF with and without the addition of molasses, WFS, and lime in soft clayey soil at $b/B=0$

Figures 12, 13 shows the pressure-settlement curves at $h/B=2.0$ for both footings ($L/B=1, 2$) for cases 2–9 compared with case 1. From these Figs. it was observed that bearing capacity of square and rectangular shaped footings declined to 72 kN/m^2 and 64 kN/m^2 for case 2 and it increased to 321 kN/m^2 and 291 kN/m^2 respectively for case 9. For case 2 at $h/B=2.0$ the improvement factor (IF) of both footings is 0.42 and for case 9 IF rises to 1.88 and 1.89 respectively, resulting in a 87% and 88% rise in ultimate bearing capacity (UBC) for both footings respectively when compared with the reference case (Fig. 14).

It can be inferred from above results that for different thickness ratios ($h/B=0.8, 1.2, 1.6,$ and 2.0) UBC of case 1 decreases when soft clayey soil layer was placed over medium dense sand (case 2) and it goes on decreasing as thickness of upper layer increases. This reduction in UBC on increasing the thickness ratio may be due to the fact that at lower $h/B=0.8$ most of the pressure is shared by the lower layer (medium dense sand) and for higher $h/B=2.0$ most of the pressure is shared by upper soft clayey soil only. But when upper layer of soft clayey soil was stabilized using

molasses, WFS, and lime the UBC and IF were increased. Also, by varying thickness of upper layer the rate of increase in the UBC of both footings ($L/B=1, 2$) is more up to $h/B=1.6$ and it lowers down at $h/B=2.0$. The difference increase in UBC of square shaped footing for case 9 by varying the thickness ratios is 21% when h/B is increased from 0 to 0.8, 17% when h/B is increased from 0.8 to 1.2, 28% when h/B is increased from 1.2 to 1.6, and 2% when h/B is increased from 1.6 to 2.0.

Effect of Aspect Ratio (L/B) on the Ultimate Bearing Capacity

In both situations (single and two-layered soil), the bearing capacity of footing with $L/B=1$ is higher than $L/B=2$, as shown in the Figs. 6, 7, 8, 9, 10, 11, 12, 13. In a single-layer soil situation, the bearing capacity determined for footing with $L/B=2$ is 11% less than that of footing with $L/B=1$. In two-layered soil situations, the bearing capacity obtained for cases 2–9 at all thickness ratio (h/B) was higher for square shaped footing with aspect ratio, $L/B=1$ than rectangular

shaped footing with aspect ratio, $L/B = 2$. When comparing the UBC obtained for case 9 for both footings, it was observed that at $h/B = 0.8$ UBC of square shaped footing ($L/B = 1$) was 5% higher than rectangular shaped footing, at $h/B = 1.2$ UBC of square shaped footing was 6% higher than rectangular shaped footing, at $h/B = 1.6$ UBC of square shaped footing was 9% higher than rectangular shaped footing, at $h/B = 2.0$ UBC of square shaped footing was 10% higher than rectangular shaped footing.

Effect of Sand Relative Density (RD) on UBC and IF

For the single sand layer and two layered soil, it can be deduced that relative density of the sand layer affected the bearing capacity of square and rectangular shaped footings. The UBC for both footings ($L/B = 1, 2$) when single layer sand provided was observed as 171 kN/m² and 154 kN/m² respectively. From the model plate load test results it was observed that for $h/B = 0.8$ and 1.2 in all the cases the UBC of both footings was greatly affected by the RD of lower layer of sand. When upper layer of soft clayey soil is placed above a layer of medium dense sand (case 2), the UBC of both footings declined, and it continues to decline as the thickness of the top layer increases. This decrease in UBC with an increase in the thickness ratio may be attributable to the fact that when the thickness ratio is lower ($h/B = 0.8, 1.2$), the majority of the pressure is distributed across the lower layer (medium dense sand), whereas when the thickness ratio is higher ($h/B = 1.6, 2.0$), the majority of the pressure is distributed across the upper soft clayey soil only. Similar trend was observed for cases 3 and 4 as IF was observed less than 1. Hence it can be inferred that for two layer (soft clay/stabilized clay over medium dense sand) situations exist, the bearing capacity of layered soil may be increased by stabilizing clayey soil and placing a sand cushion beneath the clayey layer. However to increase the bearing capacity, this sand cushion should be compacted to a high relative density.

Effect of Width Ratio (b/B) on UBC and IF

Effect of varying geogrid width ($b/B = 0, 2, 3,$ and 4) on bearing capacity improvement factor at all thickness ratios ($h/B = 0.8, 1.2, 1.6,$ and 2.0) has been discussed in this section. Figure 15 present the effect of varying the width of geogrid layer for cases 2–9 at $h/B = 1.6$ on bearing capacity IF of both footings. It may be observed that UBC and IF are increased with the placement of geogrid layer above lower layer. Also by increasing the width of geogrid UBC of both footings affected significantly. It may be observed that the performance improvement in terms of increase in IF is almost proportionate at all width ratios (b/B) except in the range of $b/B = 3$, wherein the bearing capacity improvement is much high. This is due to the fact that a geogrid mattress with a relatively narrow width functions as a deep footing and transfers the footing pressure at a wider depth, which results in an enhanced load bearing capacity as a result of higher over burden pressure. Whereas, a geogrid mattress that is relatively wider acts more like a slab, which redistributes the footing pressure over a larger area. This leads to a reduction in the intensity of the pressure that is placed on the soil, which in turn reduces the amount of settlement that occurs and increases the load carrying capacity of the footing. Also increase in UBC may be because of the mobilization of the strength that is obtained from the adhesion and interlocking of the soil-geogrid system, the base geogrid is able to withstand the downward deflection of the top layer of soft/stabilized clayey soil. Second, the geogrid layer, which is located immediately under the top layer, acts as a barrier to prevent the footing settlement from occurring thereby giving rise to a better performance improvement. The percentage increase in the UBC after $b/B = 3$ i.e. at $b/B = 4$ is low
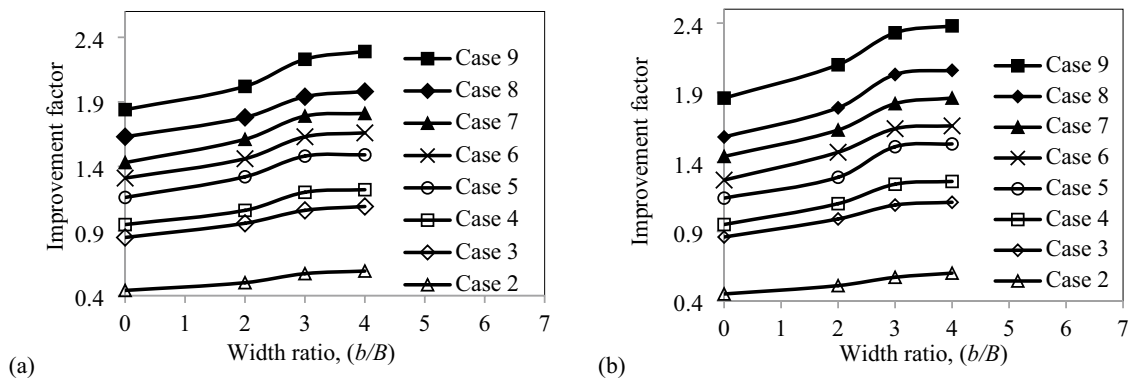

Fig. 15 Variations in improvement factor with and without geogrid layer at $h/B = 1.6$ for; (**a**) $L/B = 1$, (**b**) $L/B = 2$

and hence the optimum width of geogrid should be taken as b = 3B.

Surface Deformation

It has been shown in previous studies that the surface deformation of unreinforced soil extends from the centre of the foundation to a distance of 2.5B, and that the highest deformation typically takes place at a distance of around 1.5B from the centre of the foundation [39]. The change of surface deformation versus normalized distance from the foundation centre at thickness ratio $h/B = 1.6$ is shown in Figs. 16 and 17. In Figs. 16 and 17 positive deformation refers to the settlement of the footing, while negative deformation stands for the heave deformation of the subgrade surface. It was observed that the heave deformation at a distance of 1.5B from the centre of the foundation is higher than the uplift value at a distance of 2.5B [40]. From the model plate load test results it was observed that surface deformation for case 1 at a distance of 1.5B from the centre of both footings

($L/B = 1, 2$) was calculated as 0.48 mm and 0.53 mm respectively and at a distance of 2.5B from the centre of the both footings was calculated as 0.7 mm and 0.73 mm respectively.

The amplitude of the surface deformation increases when top layer of soft clayey soil is placed and it goes on increasing as the thickness ratio increases. When soft clayey soil is placed over medium dense sand (case 2) at thickness ratio, $h/B = 0.8$ then surface deformation at a distance of 1.5B from the centre of the square and rectangular shaped footings was increased to 0.12 mm and 0.15 mm respectively and at a distance of 2.5B from the centre of the both footings was increased to zero mm respectively. Also, by increasing the thickness ratio to $h/B = 2.0$ more heaving around the footing was noticed. At thickness ratio $h/B = 2.0$ surface deformation for case 2 at a distance of 1.5B from the centre of the both footings was increased to 0.78 mm and 0.79 mm respectively and at a distance of 2.5B from the centre of the both footings was increased to 0.14 mm. However, the amplitude of surface deformation decreases as the upper layer of soft clayey soil is stabilized with molasses, WFS, and lime. From
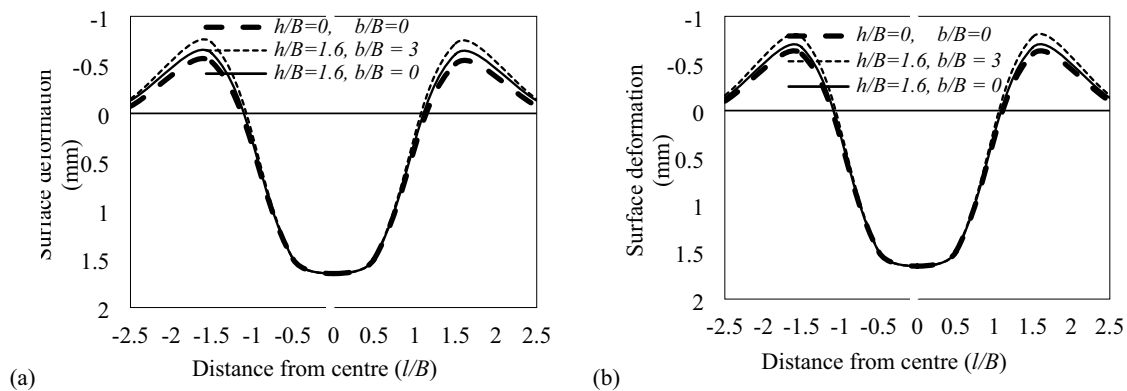

(a)   (b)

Fig. 16 Comparison of variation in heave of case 2 with case 1; (**a**) $L/B = 1$, (**b**) $L/B = 2$
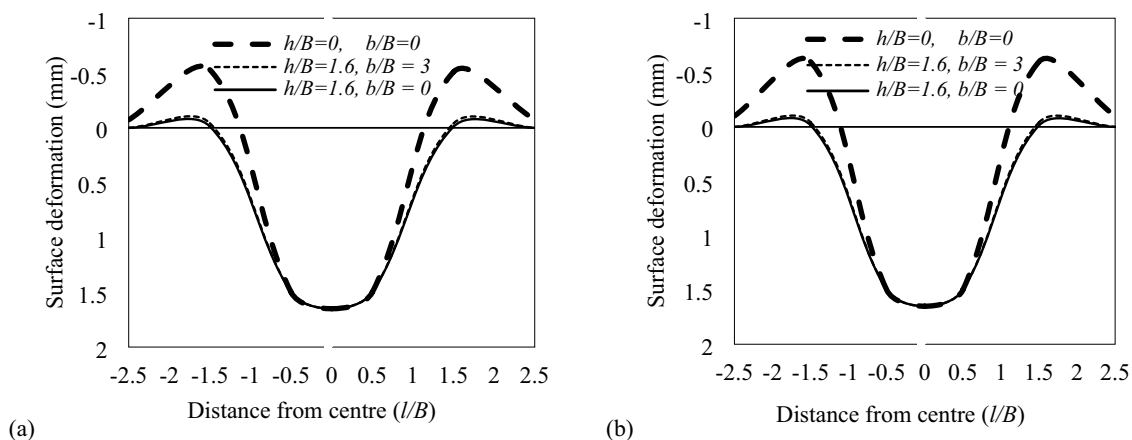

(a)   (b)

Fig. 17 Comparison of variation in heave of case 9 with case 1; (**a**) $L/B = 1$, (**b**) $L/B = 2$

the model plate load test results it was observed that while comparing the unstabilized and stabilized case 2 and case 9 at a distance of 1.5B from the centre of the both footings surface heave was reduced by 100% at $h/B = 0.8$ and 1.2, 96% and 98% at $h/B = 1.6$ and 2.0 respectively.

The placement of a geogrid layer may increase surface heave because the geogrid mattress acts more like a slab, redistributing footing pressure over a larger area and preventing settlement to reach deeper levels. As a result, the rupture surface must cover a wider area to reach the surface, increasing surface deformation in comparison to an unreinforced case. Sand offers heave resistance by mobilizing friction on the geogrid wall due to its high coefficient of friction. But in case 2, the angle of friction of soft clay was less, and the resistance to deformation is mostly based on adhesion formed at the contact, which is quite weak due to the nature of the clay. However, with the addition of molasses, WFS, and lime in to soft clayey soil the friction angle of soft clayey soil increases, and thus increasing adhesion at the interface with geogrid and sand. This leads to the conclusion that the settlement behavior of the soil profile significantly improves, which, in turn, leads to an improvement in the load bearing capacity of the soil.

Validation of Model Plate Load Tests

The finite element method is a strong investigative tool with numerous advantages over laboratory tests. However, the FEM method remains an approximation approach that idealizes real-world circumstances into a series of continuum components and using constitutive models to predict soil behavior. As a consequence, the FEM output must be validated to assure that the real-life condition is appropriately modeled. The soil strip was 500 mm long, 500 mm wide and 600 mm deep. Also, the analysis has only considered a quarter of the model (250 mm × 250 mm × 600 mm). For this study, the C3D8R element from the ABAQUS element library was employed for soil and S4R, S3 element for geogrid. C3D8R is an eight-noded linear brick with a simplified integration strategy. The water table was considered to have no effect on the bearing capacity calculation. Geotechnical properties of soft clay, stabilized clay, medium dense sand used in the FEM analysis are shown in Table 3. These parameters were calculated in laboratory using consolidated drained triaxial tests. Assembly showing placement of geogrid layer at the interface between upper and lower layer and constraints applied to the same assembly for square shaped footing at $h/B = 1.6$ are shown in Fig. 18a, b respectively.

Different numbers of meshing elements analyzed in order to find the optimum number of components. This was done in order to ensure that the findings of study would not be significantly altered by an additional increase in number of elements. Square shaped footing ($L/B = 1$) with a single reinforcing geogrid layer ($b/B = 3$) at thickness ratio (h/B) equal to 1.2 was taken into consideration for the convergence study. The size of the element was changed by increasing the number of mesh elements until a value was reached where the change in stress with increasing the number of mesh elements was found to be insignificant. For current case it was found to be somewhere in the range of 40,000.

To maintain consistency throughout the research, all models were meshed in the same way in view of the observation. Also the change in the stress corresponding to 10% settlement of the footing was seen to be roughly 5%, so the aforementioned number of elements i.e., 40,000 was chosen to be the optimum value for carrying out the work. The
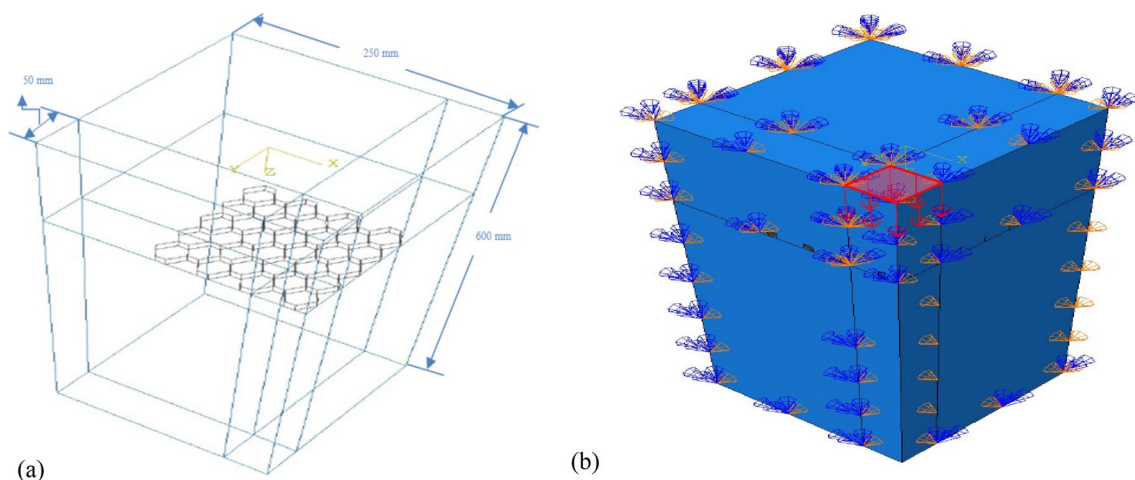

(a)   (b)

Fig. 18 (**a**) Assembly showing placement of geogrid layer at the interface between upper and lower layer; (**b**) constraints applied to the model for aspect ratio (L/B) = 1 at $h/B = 1.6$

meshing of the footing ($L/B = 1$) and geogrid are shown in Fig. 19a, b respectively.

Comparison of Experimental and Numerical Results

Using the finite element-based programme ABAQUS, pressure-settlement curves from the numerical analysis were generated, and the curves from model plate load tests were then compared. Additionally, for all the factors covered in Table 4, the UBC derived from the numerical analysis has been compared to the experimental investigation.

Figure 20 compares the pressure settlement behavior curves of case 1 for both square ($L/B = 1$) and rectangular ($L/B = 2$) shaped footings resting on homogenous sand layer observed from numerical analysis and experimental investigation. Based on the results obtained from ABAQUS software it was observed that with the addition of a soft clayey soil layer (case 2), the UBC of square and rectangular shaped footings decreased and continue to decline as the thickness ratio increased. However, after stabilizing the

soft clayey soil with molasses, WFS, and lime and placement of a geogrid layer at the interface of two layered soil resulted in an increase in UBC. The pressure settlement behavior curves produced from experimental findings and numerical analysis were compared, and the results revealed a close agreement, with numerical results slightly on the higher side. The comparison of UBC values of both square and rectangular shaped footings ($L/B = 1, 2$) observed from experimental testing and numerical analysis shows that both the values are in good agreement to each other giving coefficient of efficiency, R^2 0.99 (Fig. 21).

Displacement Contours

Displacement contours for cases 1, 2, and 9 at $b/B = 0$ and $b/B = 3$ are presented for square and rectangular shaped footings resting on homogeneous and two layered soil in Figs. 22, 23, 24 respectively. This diagram illustrates the total displacement contour, which may be used to calculate the actual displacement under load. This analysis is
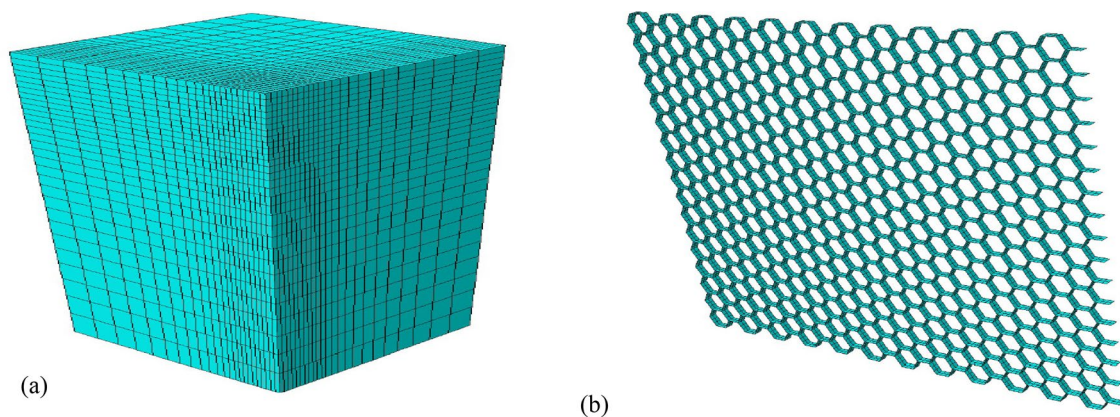

(a)

(b)

Fig. 19 Meshing applied to the models; (**a**) for aspect ratio (L/B) = 1 at h/B = 1.6; (**b**) biplanar geogrid for width ratio b/B = 3
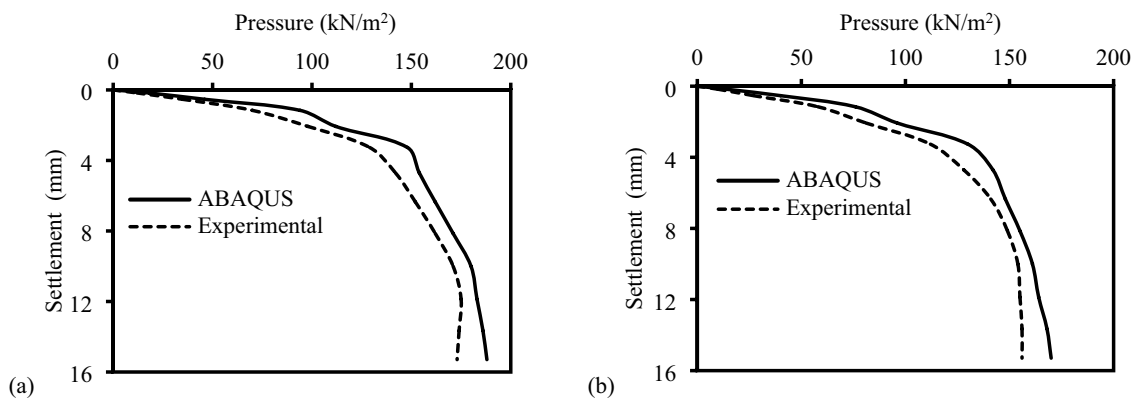

(a)

(b)

Fig. 20 Comparison of pressure-settlement curves observed from experimental and numerical analysis for case 1 at h/B = 0 for; (**a**) L/B = 1, (**b**) L/B = 2
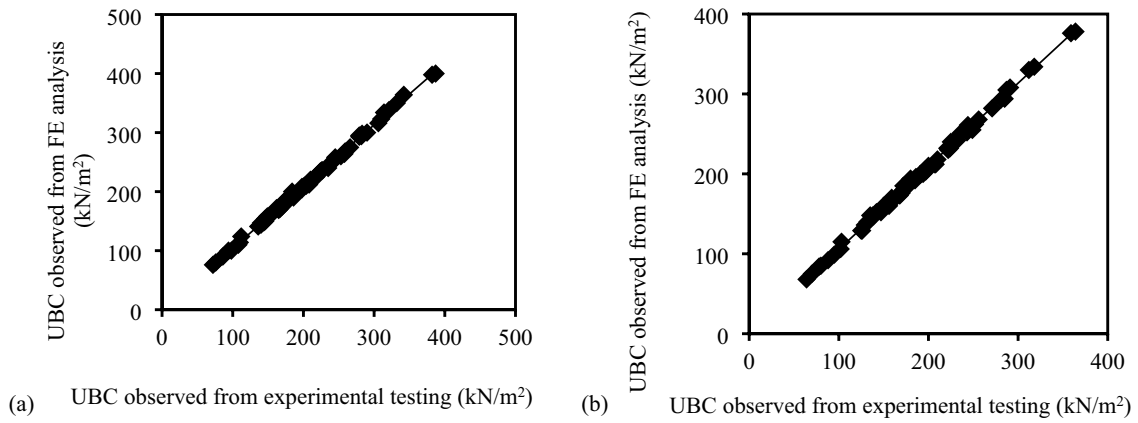
(a)   UBC observed from experimental testing (kN/m^2)

(b)   UBC observed from experimental testing (kN/m^2)

Fig. 21 Comparison of UBC observed from experimental and numerical analysis for; (**a**) $L/B = 1$; (**b**) $L/B = 2$

(a)

(b)
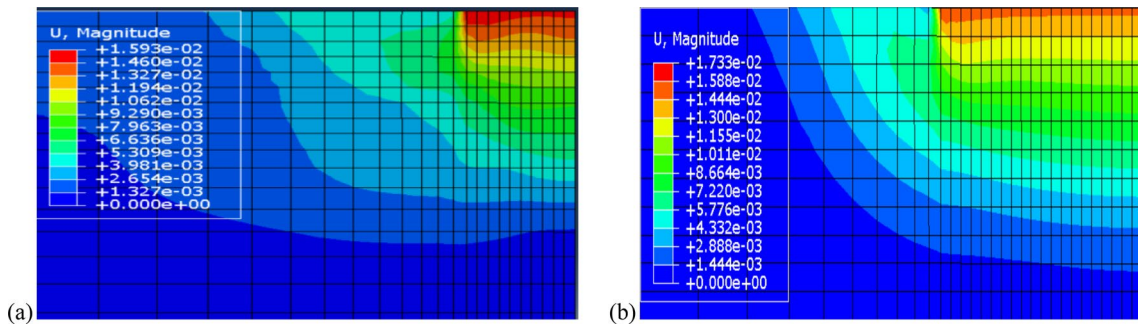
Fig. 22 Displacement value for case 1 at $h/B = 0$ and $b/B = 0$ for; (**a**) $L/B = 1$, (**b**) $L/B = 2$

(a)

(b)

(c)

(d)
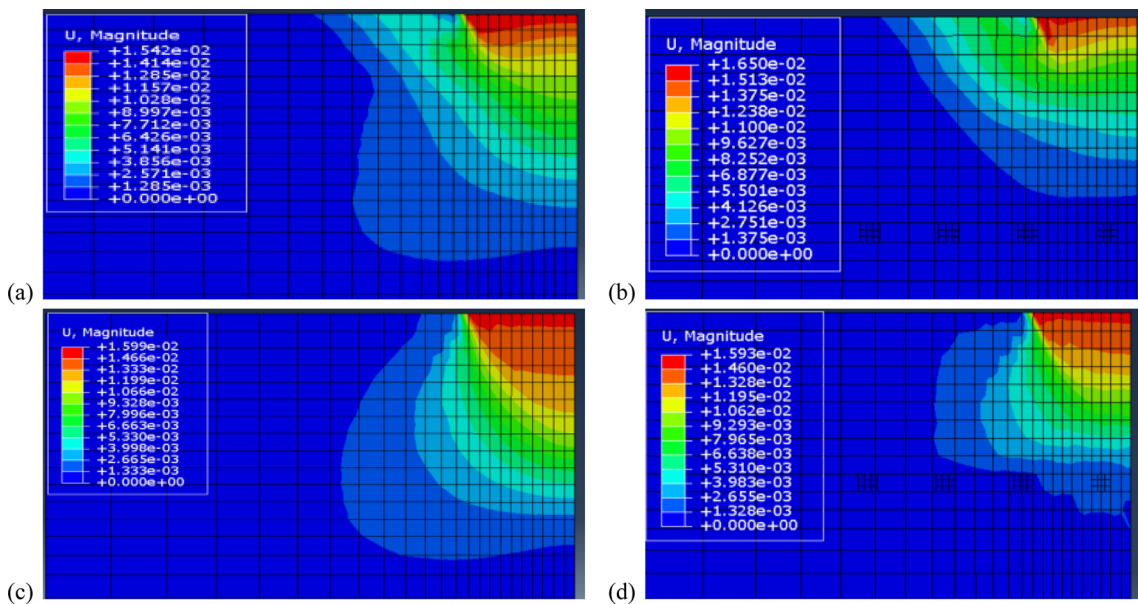
Fig. 23 Displacement value at $h/B = 1.6$ for $L/B = 1$; (**a**) case 2 at $b/B = 0$; (**b**) case 2 at $b/B = 3$; (**c**) case 9 at $b/B = 0$; and (**d**) case 9 at $b/B = 3$
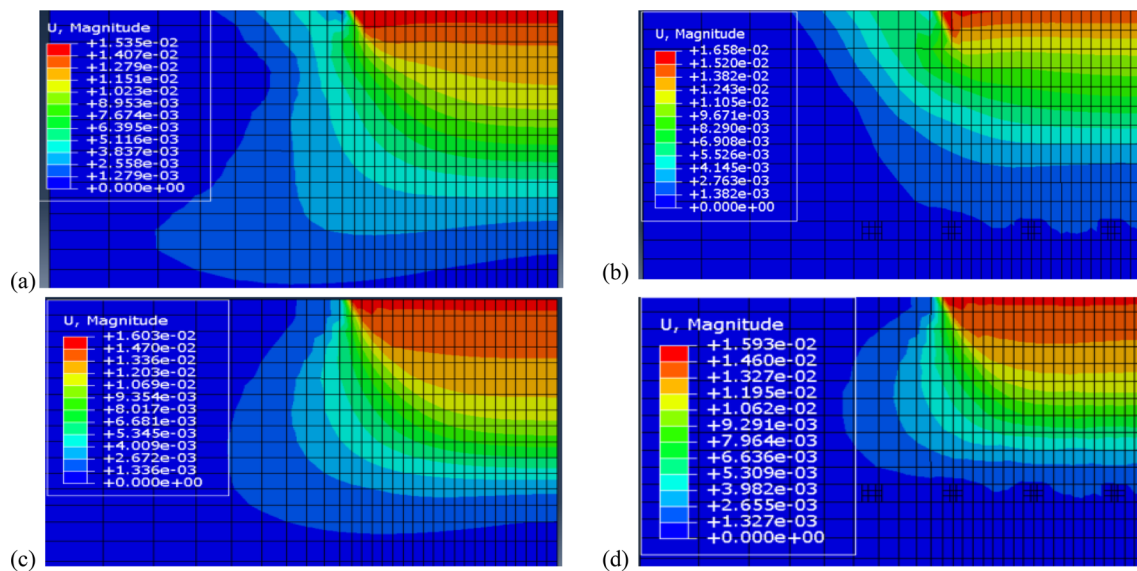
Fig. 24 Displacement value at $h/B = 1.6$ for $L/B = 2$; (**a**) case 2 at $b/B = 0$; (**b**) case 2 at $b/B = 3$; (**c**) case 9 at $b/B = 0$; and (**d**) case 9 at $b/B = 3$

required to determine if the vertical settlement of the footing design is acceptable.

Figure 22 shows that for case 1, displacement under square shaped footing is less than displacement under rectangular shaped footing; however UBC under square footing is higher than UBC under rectangular footing.

Figures 23 and 24 compared the displacement contours for case 2 and 9 with ($b/B = 3$) and without geogrid at all thickness ratios. From these figures it may be inferred that with the addition of molasses, WFS, and lime to clayey soil and the placement of a geogrid layer at the interface of two layered soils displacement under square and rectangular shaped footings is significantly reduced. In addition, after analyzing displacement contours, it is clear that the contours remained well within the specified lateral and vertical distances for the footings. This proves that the selected tank size was enough for the problem domain.

Displacement Vectors

Figures 25, 26, 27 shows the typical displacement vectors of the soil profile at all thickness ratio under square and rectangular shaped footing resting on homogeneous and two layers of soil for cases 1, 2, and 9 at $b/B = 0$ and $b/B = 3$. In Figs. 25, 26, 27 red color refers to the medium dense sand layer, while teal color refers to the soft/stabilized clayey layer.

Figure 25 shows that typical displacement vectors are observed for both footings above the surface of homogenous sand layer which refers to the formation of heave. As shown in Figs. 26 and 27 the displacement vectors for case 2 ($b/B = 0$) reaches the bottom layer of medium-dense sand for all thickness ratios ($h/B = 0.8$, 1.2, 1.6, and 2.0). However, the addition of molasses, WFS, and lime to clayey soil and the placement of a geogrid layer at the interface of two layered soils inhibit the displacement vectors with in the upper layer of stabilized clayey soil.
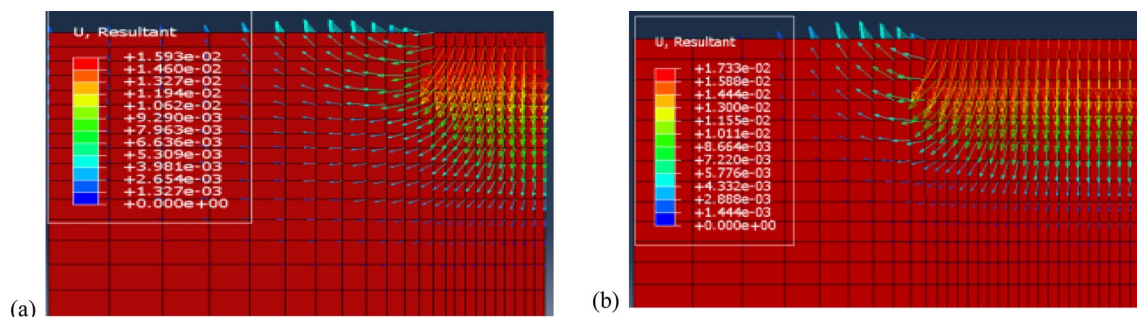

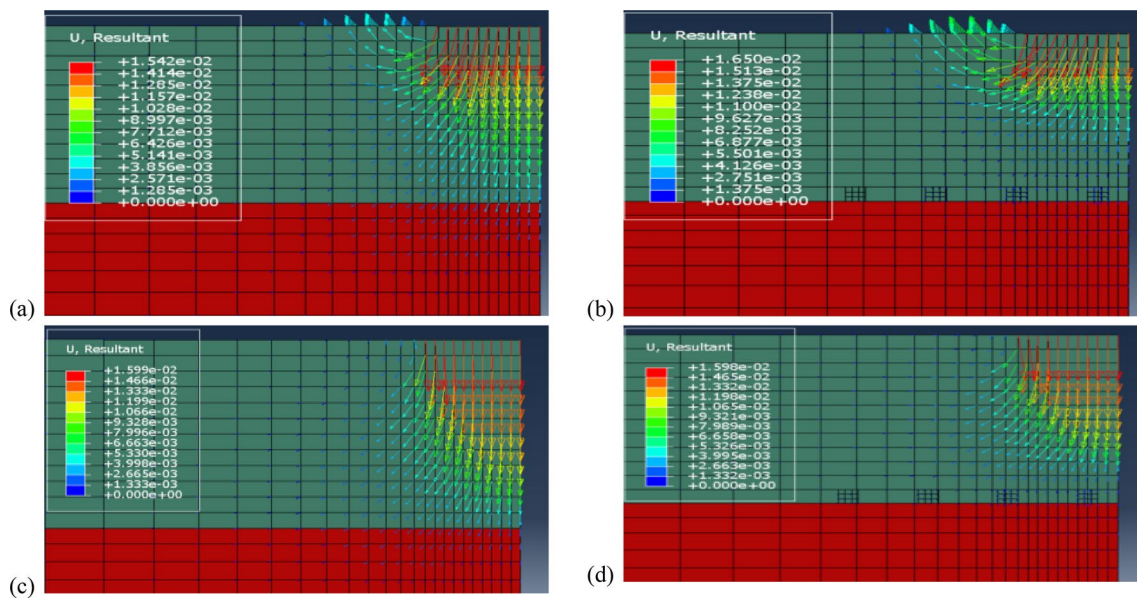**Fig. 25** Vectors of displacement at failure for case 1 at $h/B = 0$ and $b/B = 0$ for; (**a**) $L/B = 1$, (**b**) $L/B = 2$

Fig. 26 Vectors of displacement at failure for $L/B=1$ at $h/B=1.6$; (**a**) case 2 at $b/B=0$; (**b**) case 2 at $b/B=3$; (**c**) case 9 at $b/B=0$; and (**d**) case 9 at $b/B=3$
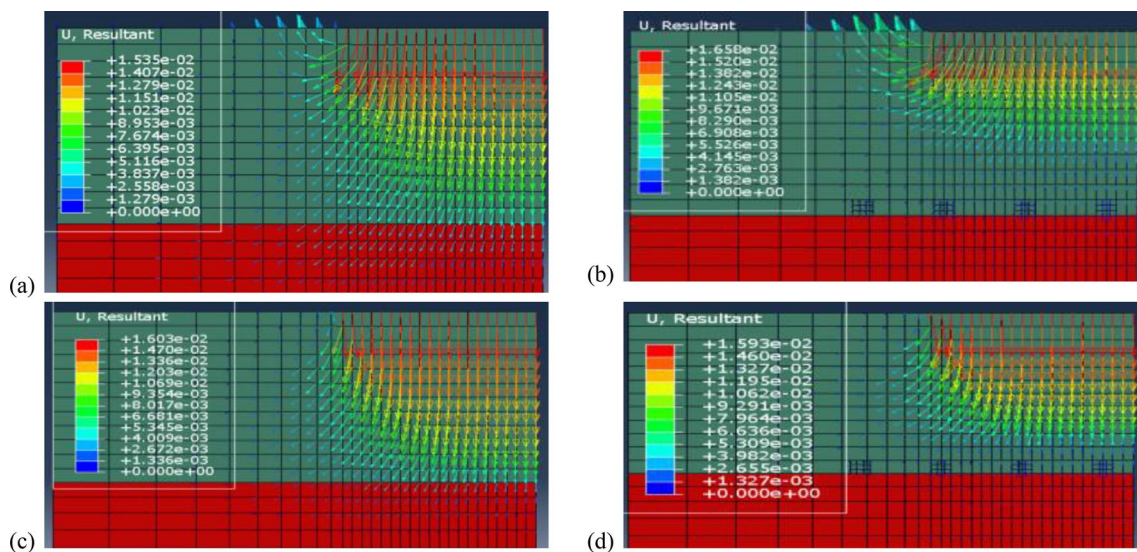

Fig. 27 Vectors of displacement at failure for $L/B=2$ at $h/B=1.6$; (**a**) case 2 at $b/B=0$; (**b**) case 2 at $b/B=3$; (**c**) case 9 at $b/B=0$; and (**d**) case 9 at $b/B=3$

Shear Strength Effect of Clay on Failure Mechanism Development

Figures 28, 29, 30 displays a plot of the results of plastic shear strain at the point of failure for cases 1, 2, and 9 at thickness ratios, $h/B=0$ and 1.6 and width ratio, b/B equals to 0 and 3. As seen in Figs. 28, 29, 30 the soil element yields gradually in the soil body from one element to the next, allowing for the formation of a shear surface.

Figures 29 and 30 demonstrates that for case 2 at $b/B=0$, when soft clayey soil is placed in upper layer beneath both type of footings then for all thickness ratios, the failure mechanism is no longer confined to the surface layer. In other words, the plastic zone does not remain confined to the upper layer for all thickness ratios at $b/B=0$; instead, it descends to the lower layers as well when upper layer is replaced by soft clayey soil. However, at thickness ratio $h/B=1.6$, the addition of molasses, WFS, and lime into clayey soil with and without inserting a geogrid layer at the
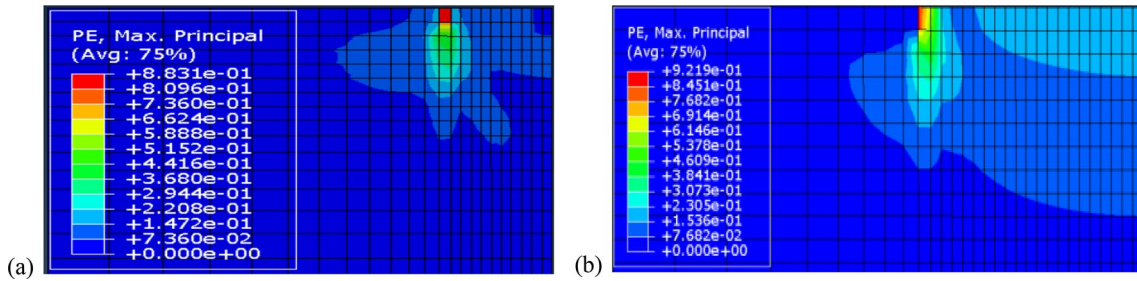
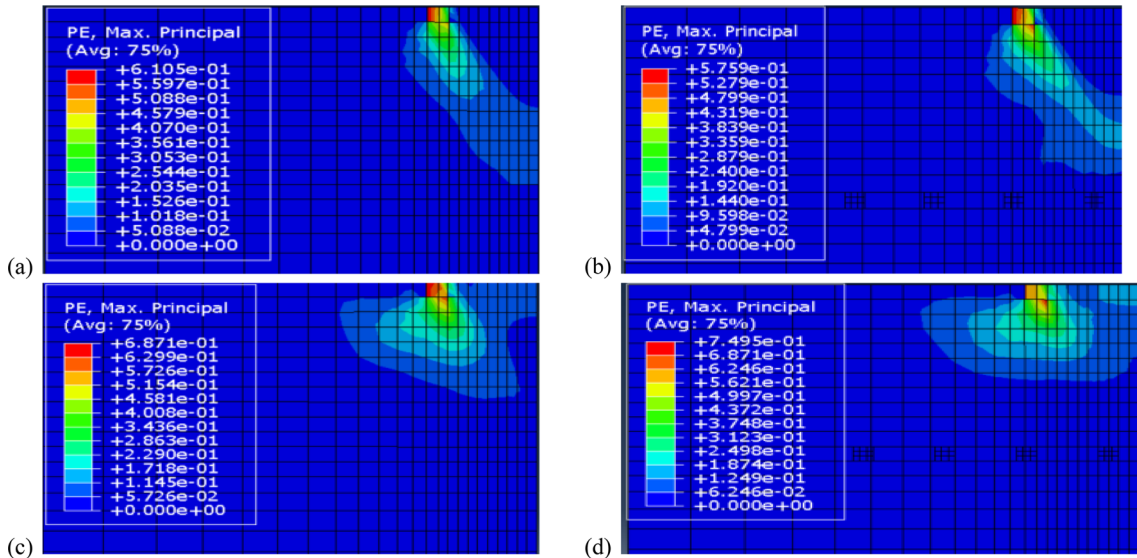**Fig. 28** Plastic strain distribution at failure point for case 1 at $h/B=0$ and $b/B=0$ for; (**a**) $L/B=1$, (**b**) $L/B=2$

Fig. 29 Plastic strain distribution at failure point under square shaped footing at $h/B=1.6$; (**a**) case 2 at $b/B=0$; (**b**) case 2 at $b/B=3$; (**c**) case 9 at $b/B=0$; and (**d**) case 9 at $b/B=3$
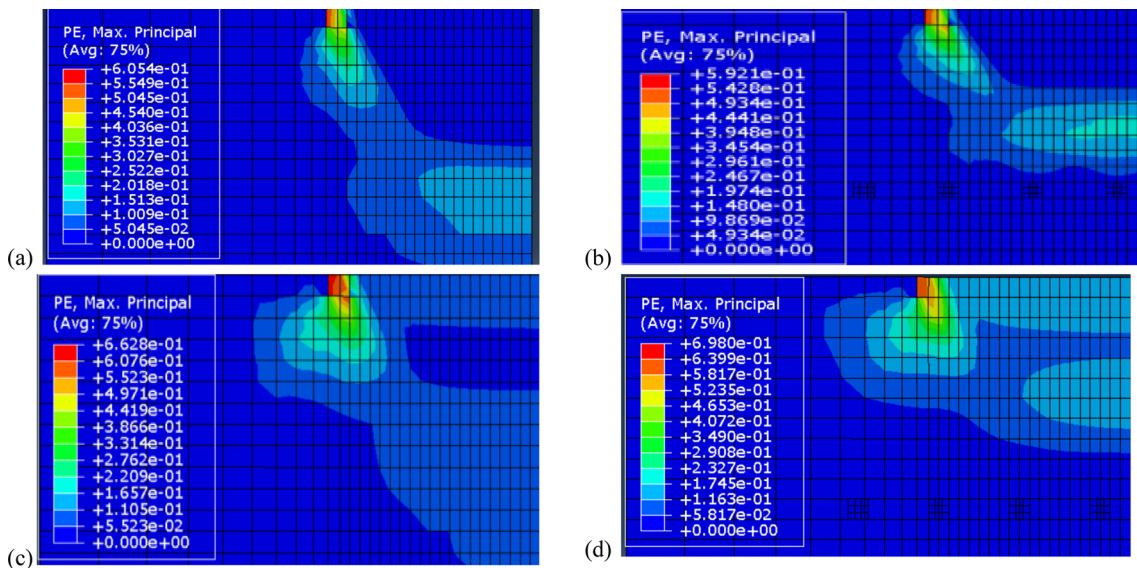

Fig. 30 Plastic strain distribution at failure point under rectangular shaped footing at $h/B=1.6$; (**a**) case 2 at $b/B=0$; (**b**) case 2 at $b/B=3$; (**c**) case 9 at $b/B=0$; and (**d**) case 9 at $b/B=3$

interface the strength of the bottom layer has no impact on the bearing capacity value since the plastic zone only persists in the top layer. Hence it can be concluded that with increasing the height of upper layer, stabilizing clayey soil with additives (molasses, WFS, and lime) and inserting a geogrid layer at the interface of two layered soil, the plastic zone tends to remain in the top layer rather of shifting to the lower layer. From previous studies it was found that as the height of the top layer rises, the plastic zone remains in the top layer rather than progressing to the lower layer [41, 42].

Conclusions

Laboratory model plate load tests were conducted to investigate the behavior of square and rectangular shaped footings resting on soft/stabilized clayey soil overlying medium dense sand with or without a geogrid layer positioned at the layered soil interface. Furthermore, numerical analysis of the same set of parameters was performed using the finite element programme ABAQUS software to validate the model plate load tests results. Following are conclusion drawn from the present research, respectively:

- For L/B equal to 1 and 2 a decrease in UBC and IF was observed for case 2 at all thickness ratios ($h/B = 0.8, 1.2, 1.6, 2.0$) when compared with reference case 1.
- An increase in the UBC and IF is observed after stabilizing the soft clayey soil layer with molasses, WFS, and lime (cases 3–9). In addition, by altering the thickness of the top layer, the rate of increase in the UBC of both footings is greater up to $h/B = 1.6$ and decreases at $h/B = 2.0$.
- The addition of a geogrid layer at the interface between a soft/stabilized clayey soil and a medium-dense sand increased the UBC and IF. It can be seen that the performance improvement in terms of increased ultimate bearing capacity was almost proportional for all width ratios (b/B) except in the range of $b/B = 3$, where the bearing capacity gain was substantially greater.
- The results of the model plate load test showed that when comparing the un-stabilized and stabilized cases 2 and 9 at a distance of 1.5B from the centre of the both footings, heave was reduced by 100% at $h/B = 0.8$ and 1.2 and 96% and 98% at $h/B = 1.6$ and 2.0 respectively.
- From model plate load test results it can be concluded that by stabilizing upper soft clayey soil with optimum percentages of additives suitable results were obtained for the UBC of square and rectangular shaped footings at $h/B = 1.6$ and $b/B = 3$ when compared with other thickness ratios (h/B) and width ratios (b/B).
- Upon comparing the pressure settlement behavior curves generated by experimental findings and numerical analysis, a close agreement was found, with numerical results rising slightly upwards.
- Displacement contours and plastic zone are found to reach the bottom layer of medium dense sand for all thickness ratios when a soft clayey soil layer is placed in the upper layer, and both are inhibited in the vicinity of the upper layer when the upper layer of soft clayey soil is stabilized with molasses, WFS, and lime, and a geogrid layer was installed.

There are various limitations to take into account for the current study effort, including scale effects, simplified soil conditions, boundary effects, and time frame effects, even if model plate load tests are carried out with more care in a controlled testing environment. These limitations can have an effect on the actual results, as the findings of laboratory model experiments may not always be directly applicable to actual situations.

Author Contributions AB contributed with the majority of the experimental and numerical investigation and writing of the manuscript. RKS reviewed the manuscript and contributed to the content and discussion.

Data Availability All data, and models used during the study appear in the published article.

Declarations

Conflict of interest The authors declare that they have no conflict of interest.

References

1. Kalantari B (2012) Foundations on expansive soils: a review. Res J Appl Sci 4(18):3231–3237
2. Chen FH (2012) Foundations on expansive soils. Elsevier, Amsterdam
3. Ikeagwuani CC, Nwonu DC (2019) Emerging trends in expansive soil stabilisation: a review. J Rock Mech Geotech Eng 11(2):423–440
4. Zamin B, Nasir H, Mehmood K, Iqbal Q, Farooq A, Tufail M (2021) An experimental study on the geotechnical, mineralogical, and swelling behavior of KPK expansive soils. Adv Civ Eng. 2:2
5. Puppala AJ, Punthutaecha K, Vanapalli SK (2006) Soil water characteristic curves of stabilized expansive soils. J Geotech Geoenviron 132(6):736–751
6. Zamin B, Nasir H, Mehmood K, Iqbal Q (2020) Field-obtained soil-water characteristic curves of KPK expansive soil and their prediction correlations. Adv Civ Eng 40:39134
7. Mallikarjuna N, Prasad KSR (2022) Performance evaluation of potassium based additives for black cotton soil stabilization. In Recent Adv Civ Eng 2:251–261
8. Zumrawi MM (2015) Construction problems of light structures founded on expansive soils in Sudan. Int J Sci Res Publ 4(8):896–902

9. Salahuddin S, Quareshi S (2018) Adverse impact of canal irrigation on the environment in hyper arid parts of the indian desert. Natl Geogr J India 64(3–4):180–187

10. Gourley CS, Newill D, Schreiner HD (1993) Expansive soils: TRL's research strategy. In Proc. 1st Int. Symposium on Engineering Characteristics of Arid Soils, London

11. Nelson J, Miller DJ (1997) Expansive soils: problems and practice in foundation and pavement engineering. John Wiley and Sons

12. Thomas PJ, Baker JC, Zelazny LW (2000) An expansive soil index for predicting shrink–swell potential. Soil Sci Soc Am J 64(1):268–274

13. Jones DE Jr, Holtz WG (1973) Expansive soils—the hidden disaster. ASCE 43(8):49–51

14. Jones LD, Jefferson I (2012) Expansive soils. ICE manual of geotechnical engineering. ICE Publishing, London: 413–41. 40

15. Bhardwaj A, Sharma RK (2022) Designing thickness of subgrade for flexible pavements incorporating waste foundry sand, molasses, and lime. Innov Infrastruct Solut 7(1):1–18

16. Sanoop G, Cyrus S, Abraham BM (2021) Improvement of geotechnical properties of marine clay using waste foundry sand. Adv Sustain Constr Mat 2:361–368

17. Zhang Y, Sappinen T, Vilenius M, Korkiala-Tanttu L (2021) Investigations into stabilized structures with the use of waste foundry sand. In IOP Conf Series: EES 710(1):012028

18. Malanda N, Mfoutou NN, Madila EEN, Louzolo-Kimbembe P (2022) Microstructure of fine clay soils stabilized with sugarcane molasses. Open J Civ Eng 12(2):247–269

19. Achal D (2022) Evaluating the durability of expansive subgrade soils stabilized with molasses and cement. Doctoral dissertation, Makerere University.

20. Jiménez JE, Fontes Vieira CM, Colorado HA (2022) Composite soil made of rubber fibers from waste tires, blended sugar cane molasses, and kaolin clay. Sustainability 14(4):2239

21. Zami MS, Ewebajo AO, Al-Amoudi OSB, Al-Osta MA, Mustafa YMH (2022) Compressive strength and wetting-drying cycles of al-hofuf hamrah soil stabilized with cement and lime. Arab J Sci Eng 2:1–16

22. Omid A, Mojtaba G (2022) Geotechnical properties of lime-magnesium slag stabilized clayey sand: experimental study. Arab J Sci Eng 47(10):13673–13685

23. Ansari MA, Roy LB (2022) Bearing capacity of a circular footing resting on geogrid reinforced foundation: an experimental and neuro-fuzzy based model. Int J Performability Eng 18(10):2

24. Useche-Infante D, Aiassa Martinez G, Arrúa P, Eberhardt M (2022) Experimental study of behaviour of circular footing on geogrid-reinforced sand. Geomech Geoeng 17(1):45–63

25. Zhu Y, Zhang F, Jia S (2022) Embodied energy and carbon emissions analysis of geosynthetic reinforced soil structures. J Clean Prod 370:133510

26. Chaudhary B, Hazarika H, Murakami A, Fujisawa K (2018) Mitigation of earthquake-induced damage of breakwater by geogrid-reinforced foundation. Mar Georesour Geotechnol 36(7):827–840

27. Mohammed SA, Naimi S, AbdulKareem AH (2022) The effect of geogrid reinforcement of embankment over soft foundation. Period Eng Nat Sci 10(6):5–27

28. Shakir RR, Jawad ZH (2022) Bearing capacity of shallow foundation on geogrid reinforced soil. In AIP Conf Proc 2660(1):020123

29. Akbar A, Bhat JA, Mir BA (2021) Plate load tests for investigation of the load–settlement behaviour of shallow foundation on bitumen-coated geogrid reinforced soil bed. Innov Infrastruct Solut 6(2):1–17

30. ASTM 2004 Standard test methods for particle size distribution of soils. ASTM D6913–04. Pennsylvania, PA, USA

31. ASTM 2011 Standard practice for classification of soils for engineering purposes (unified soil classification system). ASTM D2487–11. Pennsylvania, PA, USA

32. ASTM 2016 Standard Test Methods for Maximum Index Density and Unit Weight of Soils Using a Vibratory Table. ASTM D4253–16. West Conshohocken, PA, USA

33. ASTM 2016 Standard Test Methods for Minimum Index Density and Unit Weight of Soils and Calculation of Relative Density. ASTM D4254–16. West Conshohocken, PA, USA

34. ASTM 2010 Standard test methods for liquid limit, plastic limit, and plasticity index of soils. ASTM D4318–10. West Conshohocken, PA, USA

35. ASTM 2010 Standard test methods for specific gravity of soil. ASTM D854–10. Pennsylvania, PA, USA

36. BIS 1977 Determination of free swell index of soil. IS:2720 Part 40. New Delhi, India

37. ASTM 2007 Standard test methods for laboratory compaction characteristics of soil using standard effort ($12400 ftlbf/ft^3 (600 kN$-m/m^3)). ASTM D698–07e1. West Conshohocken, PA, USA

38. BIS 1982 Method of Load test on Soil. IS: 1888. New Delhi, India

39. Harikumar M, Sankar N, Chandrakaran S (2016) Behaviour of model footing resting on sand bed reinforced with multi-directional reinforcing elements. Geotext Geomembr 44(4):568–578

40. Yin JH, Fang Z (2010) Physical modeling of a footing on soft soil ground with deep cement mixed soil columns under vertical loading. Mar Georesour Geotechnol 28(2):173–188

41. Potts DM, Zdravkovic L (2001) Finite element analysis in geotechnical engineering: application. Thomas Telford

42. Zhu M (2004) Bearing capacity of strip footings on two-layer clay soil by finite element method. ABAQUS Users Conf, Boston